Supporting information

Theoretical search of a simple characteristic for Long-lived Organic Room-Temperature Phosphorescence materials with H-aggregation

*Jing Gao, [‡a] Yuanyuan Zhao, [‡a] Xiaoxia You, [a] Yun Geng,[*a] Guogang Shan,[*a] Zhongmin Su[*b] and Ying Gao[c]*

[a]Institute of Functional Material Chemistry, Faculty of Chemistry, Northeast Normal University, Changchun 130024, Jilin, P. R. China; Email: gengy575@nenu.edu.cn; shangg187@nenu.edu.cn

[b]College of Chemistry, Jilin University, Changchun 130012, Jilin, P. R. China; Email: zmsu@nenu.edu.cn

[c]Jilin Engineering Normal University, Changchun 130052, Jilin, P. R. China

‡*Authors contributed equally to this paper.*

Table of contents

1. Computational details

2. Supplementary Schemes and Figures

Figure S1. The simulated absorption spectra of TXCL dimer (black line) and TXOME dimer (red line) together with experimental spectra of TXCL and TXOME crystals (dotted lines).

Figure S2. The calculated excited energy levels of the monomers and dimers.

Figure S3. The amount of transferred charge (χ) and charge density difference (CDD) maps for the $S_0 \rightarrow S_1$ transition where the green and purple colors presents the decrease and increase in the electron density, respectively.

Figure S4. The calculated SOC values of the monomers and dimers.

Figure S5. The relevant parameters of the parent dimers (orange color) and dimers of TX derivatives (green color) including (a) the oscillator strengths of S_1 state, (b) the maximum oscillator strengths in singlet states, (c) the numbers of ISC channels, (d) the maximum SOC, and (e) the BSSE corrected intermolecular interaction energy.

Table S1. The calculated oscillator strengths of the monomers and dimers for $S_0 \rightarrow S_1$ transition and the corresponding difference ($\triangle$) in the TX-derivatives.

Table S2. The energy transfer rate (s^{-1}) of dimers in the TX-derivatives.

Table S3. The calculated electronic couplings (meV) of dimers in the TX-derviatives for energy transfer.

Table S4. The calculated reorganization energies (eV) of the dimers in the TX-derivatives for energy transfer.

Table S5. The calculated electronic couplings (meV), reorganization energies (eV) and electron transfer rates (s^{-1}) of dimers in the TX-derivatives for electron transfer.

Table S6. The experimental phosphorescence lifetimes and phosphorescent quantum efficiencies of the TX derivatives.

Table S7. The slipping angles of the dimers at S_1 states in CNPh derivatives.

Table S8. The vertical distances of the dimers at S_0 states in CNPh derivatives.

3. References

1. Computational details

All studied geometrical, electronic structures and relevant photophysical property were explored by the Gaussian 16,[1] ADF 2016[2] and Multiwfn 3.8[3] program packages. We used different combinations of basis set for heavy atoms and main group atoms. The "double-ξ" quality basis set LANL2DZ[4] were selected as the basis set for I atom. The 6-311G* basis set was employed for the other atoms.

The monomers and dimers selected from the experimental crystals were optimized using B3LYP functional and B3LYP-D3, respectively. Meanwhile, the calculated UV/Vis absorption spectrums of dimers using the B3LYP-D3 functional are matching the experimental spectrums which are shown in Figure S1. Hence we selected the B3LYP-D3 functional to calculate the related properties of the selected dimers. Using Quantum Mechanics/Molecular Mechanics (QM/MM) method[5] which considers the intermolecular interaction effects to optimize the geometrical structures. The chosen monomers and dimers were calculated at the QM level and the surrounding molecules are treated at MM level. The density functional theory (DFT) and time-dependent density functional theory (TDDFT)[6] were selected for central molecules in ground states and excited states, respectively. The universal force field (UFF)[7] were used to calculate the surrounding molecules. The spin-orbital coupling (SOC) matrix element values of the monomers and dimers were calculated by the ADF 2016 program package with the ZORA/DZP basis set.[8] B3LYP functional and B3LYP-D3 functional were used to calculate the SOC values for the monomers and dimers, respectively. The software Multiwfn 3.8[3] was used to calculate the amount of charge transfer and perform the charge density difference (CDD) maps.[9]

The semiempirical Marcus formula which is employed to calculate the energy transfer rate and electron transfer rate between the nearest neighboring molecules could be expressed as:

$$k = \sqrt{\frac{4\pi^3}{h^2 \lambda k_B T}} |V_{HG}|^2 \exp\left(-\frac{(\Delta G + \lambda)^2}{4\lambda k_B T}\right) \qquad (1)$$

Where T is temperature, λ is the reorganization energy, V_{HG} represents electronic coupling, ΔG denotes the Gibbs free energy difference, h is Planck constant, and k_B is Boltzmann constants. The value of Gibbs free energy difference (ΔG) in the formula (1) is zero since the same structures of dimers whether in ground states or excited states.

For the energy transfer, we used the TDDFT[6] method at the B3LYP-D3/6-311G* level to calculate the electronic coupling for energy transfer between the molecules in dimers by Gaussian 16 software.[1] The origin of the different contribution to excitation energy transfer (EET) coupling could be expressed as:

$$V = V^{CC} + V^{TB} \qquad (2)$$

Where V^{CC} contains the Coulomb and exchange integrals which are corresponding to the terms seen in Förster and Dexter formulations, V^{TB} contains the coupling related to the involvement of ionic configurations. The reorganization energy (λ) in the formula (1) can be calculated by Nelson's four-point method:

$$\lambda = \lambda_1(Dimer) + \lambda_2(Dimer) = \left[E\left(^3H_{fc}\right) - E\left(^3H_{opt}\right)\right] + \left[E\left(^1G_{fc}\right) - E\left(^1G_{opt}\right)\right] \qquad (3)$$

The subscripts opt and fc in the formula (3) represent optimized states and Franck-Condon excited states, respectively.

For the electron transfer, the electronic coupling V_{eff} calculated by the site-energy corrected method in ADF 2016 program package[8] could be expressed as:

$$V_{eff} = \frac{J_{12} - \frac{1}{2}(e_1 + e_2)S_{12}}{1 - S_{12}^2} \tag{4}$$

Where J_{12} and S_{12} represent the direct charge transfer integral and overlap integral between the LUMOs of molecule 1 and 2, respectively. And e_1 and e_2 represent their respective site energies. The reorganization energy (λ) in the formula (1) can be calculated by the adiabatic potential surfaces which were proposed by Sunto[10]:

$$\lambda_{int} = \lambda_1(H) + \lambda_2(G) = \left[E(H^-) - E(H) \right] + \left[E(G) - E(G^+) \right] \ldots\ldots\ldots\ldots \tag{5}$$

Where $E(G^+)$ and $E(G)$ represent the energies of the neutral dimer at the anionic geometry and optimal ground-state geometry, and $E(H)$ and $E(H^-)$ represent the energies of the radical cation at the neutral geometry and optimal cation geometry.

The intermolecular interactions between the calculated dimers are performed by Multiwfn 3.8[3] with Independent Gradient Model (IGM) method[11] and plotted by visual molecular dynamics (VMD) package.[12] The IGM model which is founded on electron density (ED)-based methodology could be used to identify and quantify non-covalent interaction analyses. The interaction regions are defined by a descriptor δg^{inter} using an intra/inter uncoupling scheme:

$$g^{inter}(r) = \left| \sum_A \sum_{i \in A} \nabla \rho_i(r) \right| \tag{6}$$

$$g^{IGM,inter}(r) = \left| \sum_A abs \left[\sum_{i \in A} \nabla \rho_i(r) \right] \right| \tag{7}$$

$$\delta g^{\text{inter}}(r) = g^{\text{IGM,inter}}(r) - g^{\text{inter}}(r) \tag{8}$$

The subscript A in formulas (6) and (7) represents fragment number. $\nabla\rho$ is the different pro-molecular atomic ED gradient components. The subscript i represents the atomic number.
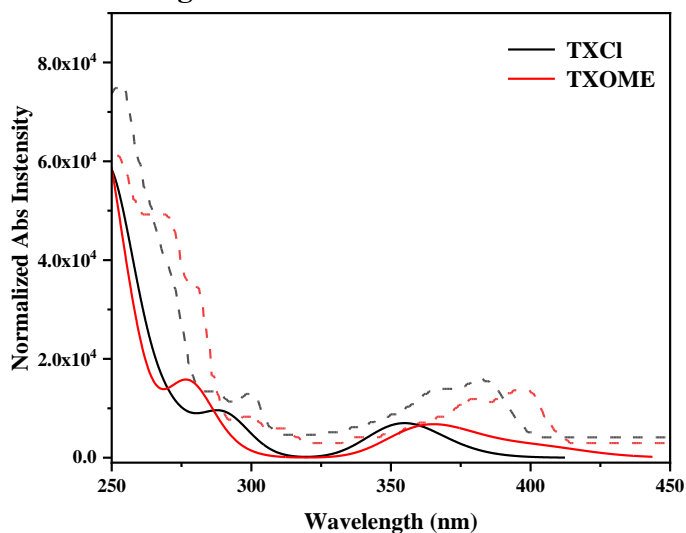
2. Supplementary Schemes and Figures

Fig. S1 The simulated absorption spectra of TXCL dimer (black line) and TXOME dimer (red line) together with the experimental spectra of TXCL and TXOME crystals (dotted lines)
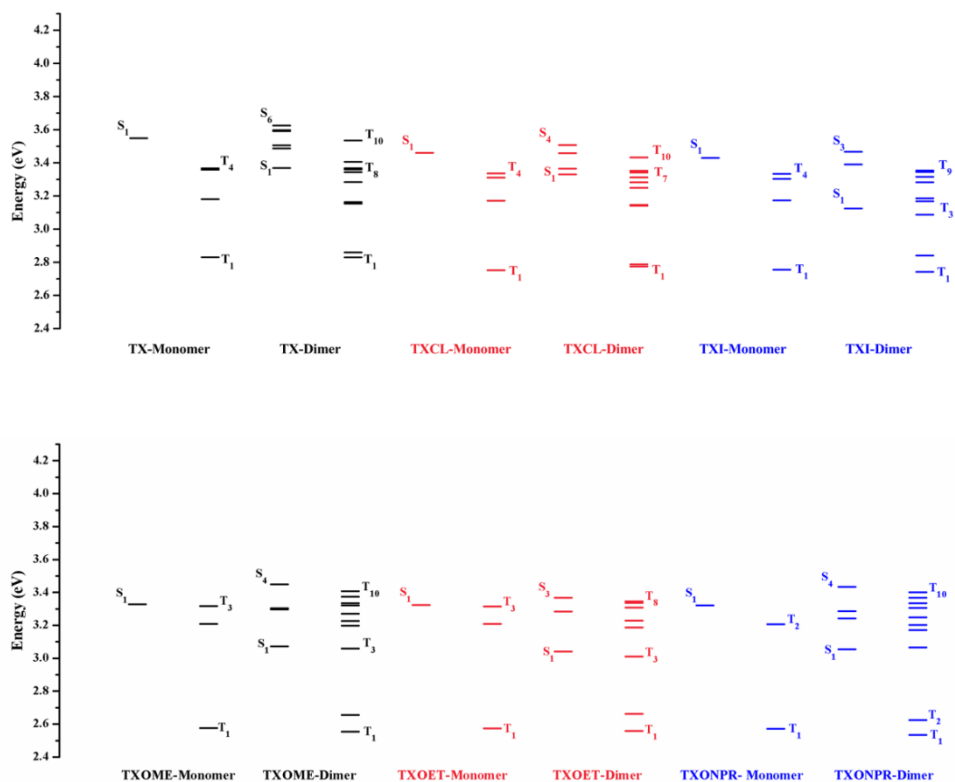
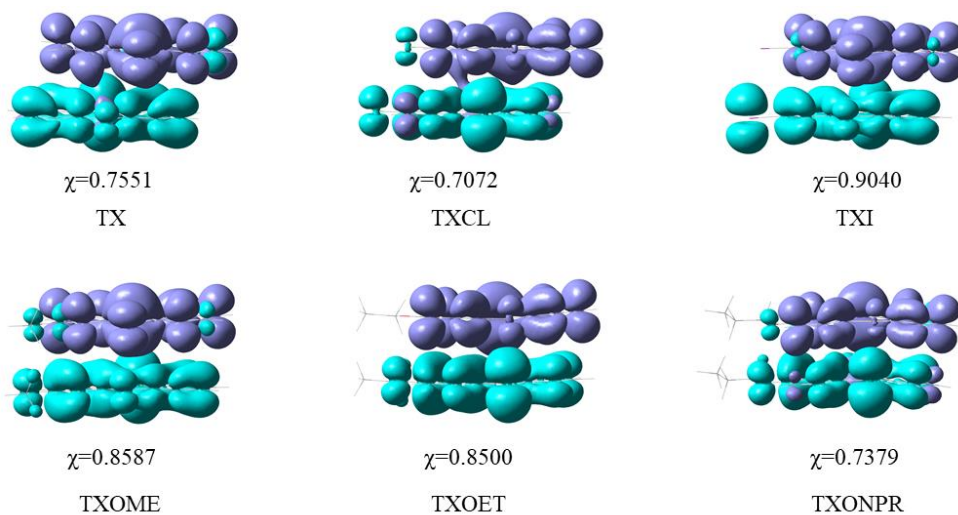**Fig. S2** The calculated excited energy levels of the monomers and dimers.
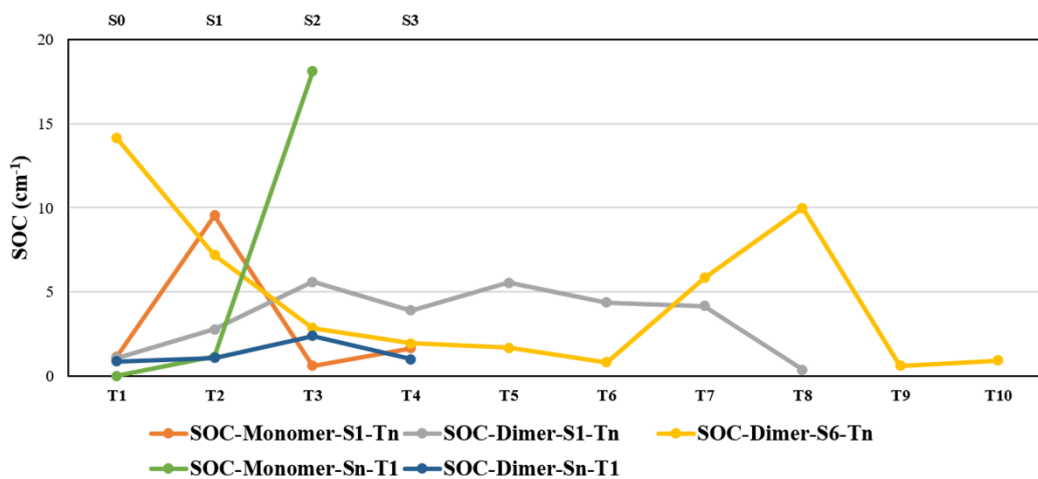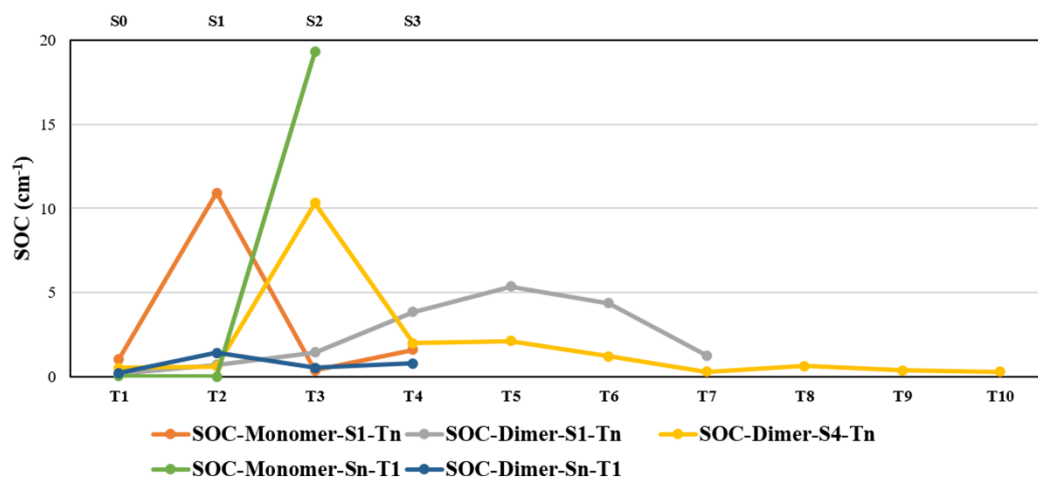

Fig. S3 The amount of transferred charge (χ) and charge density difference (CDD) maps of all studied dimers for the $S_0{\rightarrow}S_1$ transition where the green and purple colors present the decrease and increase in the electron density, respectively.
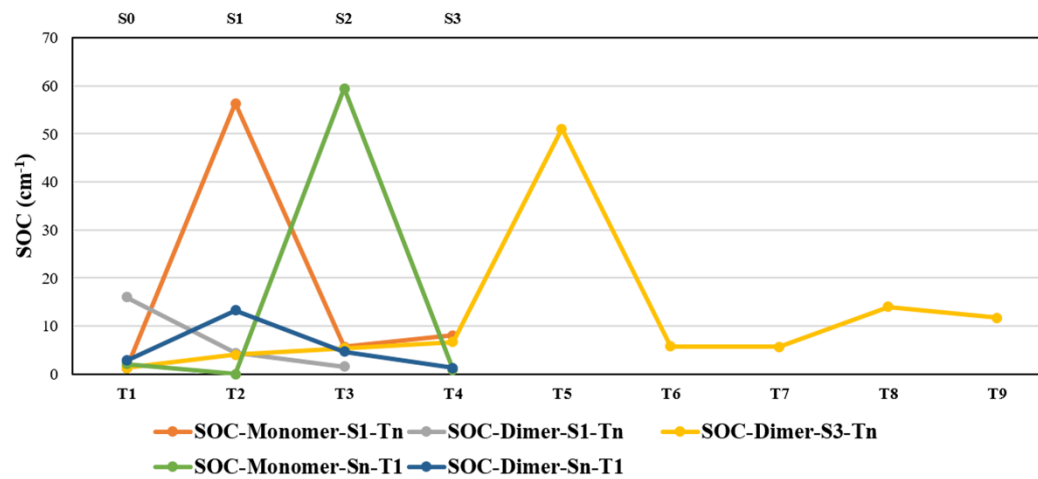
TX S_n-T_n SOC

TXCL S_n-T_n SOC

TXI S_n-T_n SOC

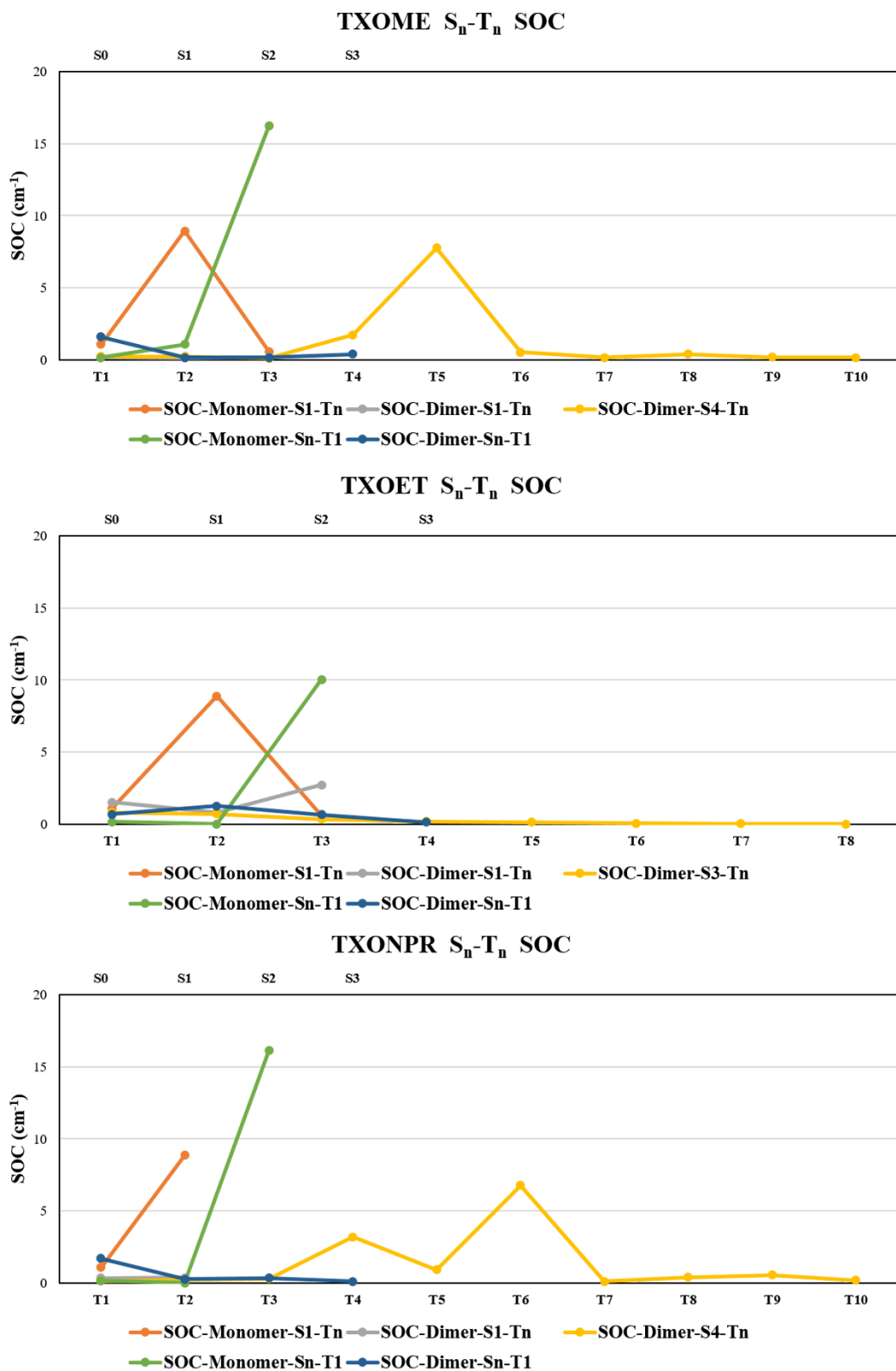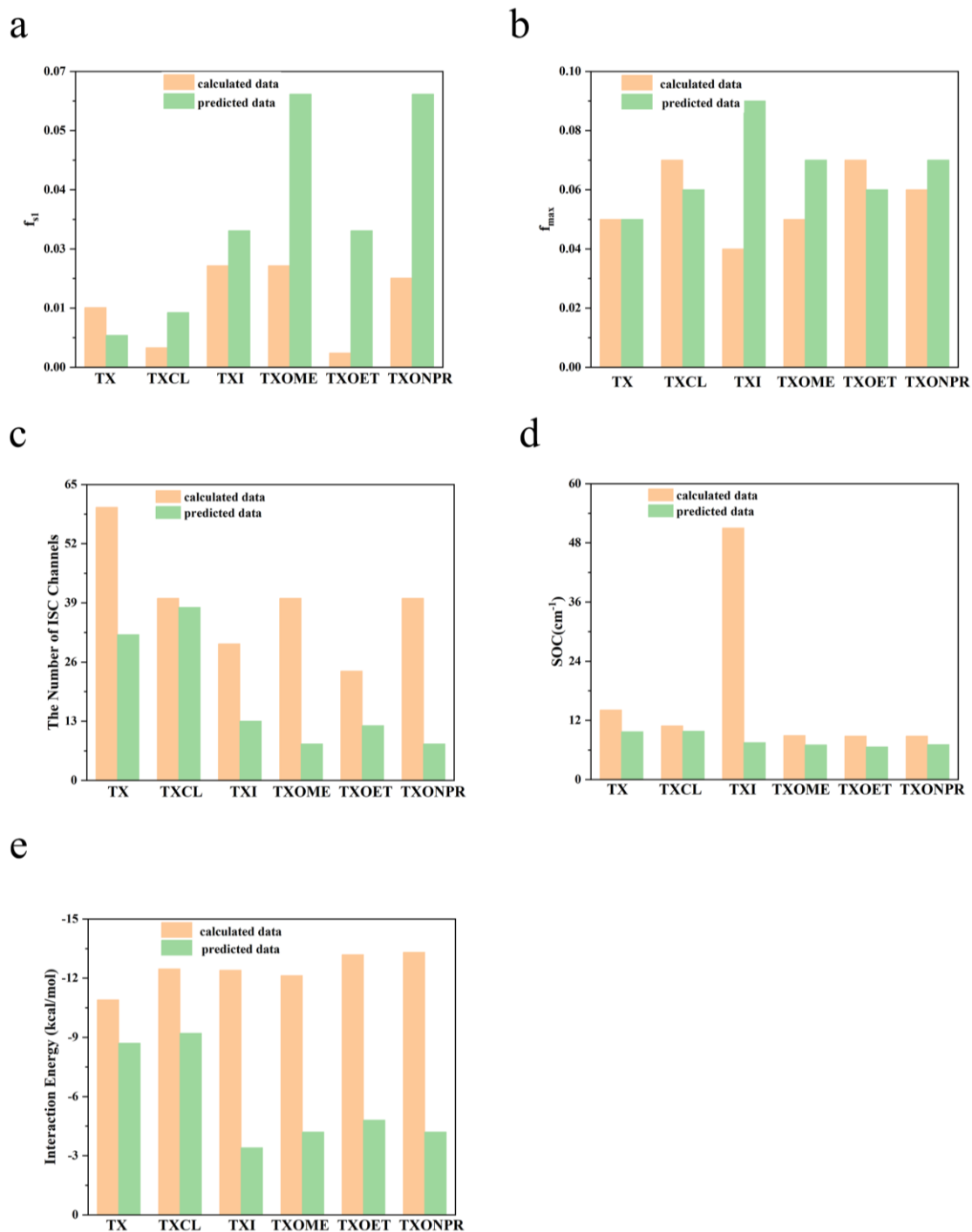**Fig. S4** The calculated SOC values of the monomers and dimers.

Fig. S5 The relevant parameters of the parent dimers (orange color) and dimers of TX derivatives (green color) including (a) the oscillator strengths of S_1 state, (b) the maximum oscillator strengths in singlet states, (c) the numbers of ISC channels, (d) the maximum SOC, and (e) the BSSE corrected intermolecular interaction energy.

Table S1. The calculated oscillator strengths of the monomers and dimers for $S_0 \rightarrow S_1$ transition and the corresponding difference ($\triangle$) in the TX-derivatives.

Dimer	Monomer	Dimer	$\triangle$
TX	0.0611	0.0131	0.0480
TXCl	0.0579	0.0043	0.0536
TXI	0.0525	0.0223	0.0302
TXOME	0.0622	0.0223	0.0399
TXOET	0.0615	0.0031	0.0584
TXONPR	0.0611	0.0196	0.0415

Table S2. The energy transfer rate (s^{-1}) of dimers in the TX-derivatives.

Dimer	S_1-S_1	T_1-T_1
TX	5.12E+07	4.06E+12
TXCl	5.77E+08	7.72E+12
TXI	7.22E+08	3.69E+11
TXOME	4.27E+08	2.74E+11
TXOET	2.28E+08	3.26E+11
TXONPR	2.79E+08	3.85E+10

Table S3. The calculated electronic couplings (meV) of dimers in the TX-derviatives for energy transfer.

Dimer	S_1-S_1	T_1-T_1
TX	3.35E-02	4.45E+02
TXCl	3.29E-02	4.45E+02
TXI	-1.59E-02	-2.54E+02
TXOME	-2.01E-02	-2.73E+02
TXOET	-2.52E-02	-3.16E+02
TXONPR	2.03E-02	2.82E+02

Table S4. The calculated reorganization energies (eV) of the dimers in the TX-derivatives for energy transfer.

Dimer	S_1-S_0	T_1-S_0
TX	0.86	0.28
TXCl	0.62	0.23
TXI	0.46	0.40
TXOME	0.55	0.44
TXOET	0.66	0.45
TXONPR	0.60	0.63

Table S5. The calculated reorganization energies (eV), electronic couplings (meV) and electron transfer rate (s^{-1}) of dimers in the TX-derivatives for electron transfer.

Dimer	Reorganization Energies (eV)	Electronic Couplings (meV)	Electron Transfer Rate (s-1)
TX	1.25	3.11E-02	8.52E+05
TXCl	1.82	4.08E-02	4.75E+03
TXI	1.83	3.37E-03	2.94E+01
TXOME	1.27	1.94E-02	2.69E+05
TXOET	1.26	3.23E-03	8.19E+03
TXONPR	1.26	5.41E-02	2.33E+06

Table S6. The experimental phosphorescence lifetimes and phosphorescent quantum efficiencies of the TX derivatives.

	Φ_{RTP}(%)	τ_{RTP}(ms)
TX	0.90	0.84
TXCl	74.7	2.10
TXI	0.10	0.40
TXOME	11.7	0.74
TXOET	1.40	0.25
TXONPR	1.30	0.21

Table S7. The slipping angles of the dimers at S_1 states in CNPh derivatives.

	oCNPh	mCNPh	pCNPh	TCNPh
Slipping angle	88.3°	82.0°	82.3°	88.4°

Table S8. The vertical distances of the dimers at S_0 states in CNPh derivatives.

	oCNPh	mCNPh	pCNPh	TCNPh
Vertical distance	3.553 Å	3.495 Å	3.409 Å	3.359 Å

3. References

1   M. J. Frisch, G. W. Trucks, H. B. Schlegel, G. E. Scuseria, M. A. Robb, J. R. Cheeseman, G. Scalmani, V. Barone, G. A. Petersson, H. Nakatsuji, X. Li, M. Caricato, A. V. Marenich, J. Bloino, B. G. Janesko, R. Gomperts, B. Mennucci, H. P. Hratchian, J. V. Ortiz, A. F. Izmaylov, J. L. Sonnenberg, D. Williams-Young, F. Ding, F. Lipparini, F. Egidi, J. Goings, B. Peng, A. Petrone, T. Henderson, D. Ranasinghe, V. G. Zakrzewski, J. Gao, N. Rega, G. Zheng, W. Liang, M. Hada, M. Ehara, K. Toyota, R. Fukuda, J. Hasegawa, M. Ishida, T. Nakajima, Y. Honda, O. Kitao, H. Nakai, T. Vreven, K. Throssell, J. A. Montgomery, J. E. Peralta, F. Ogliaro, M. J. Bearpark, J. J. Heyd, E. N. Brothers, K. N. Kudin, V. N. Staroverov, T. A. Keith, R. Kobayashi, J. Normand, K. Raghavachari, A. P. Rendell, J. C. Burant, S. S. Iyengar, J. Tomasi, M. Cossi, J. M. Millam, M. Klene, C. Adamo, R. Cammi, J. W. Ochterski, R. L. Martin, K. Morokuma, O. Farkas, J. B. Foresman and D. J. Fox, Gaussian 16, Revision B.01, Gaussian Inc., Wallingford CT, 2016.
2   ADF, SCM, Theoretical Chemistry, Virje Universiteit, Amsterdam, The Netherlands, 2016.
3   T. Lu and F. W. Chen, *J. Comput. Chem.*, 2012, **33**, 580.
4   P. J. Hay and W. R. Wadt, *J. Chem. Phys.*, 1985, **82**, 270.
5   M. C. Li, M. Hayashi and S. H. Lin, *J. Phys. Chem. A*, 2011, **115**, 14531.
6   M. E. Casida, C. Jamorski, K. C. Casida and D. R. Salahub, *J. Chem. Phys.*, 1998, **108**, 4439.
7   Y. C. Duan, Y. Wu, J. L. Jin, D. M. Gu, Y. Geng, M. Zhang and Z. M. Su, *Chem. Phys. Chem.*, 2017, **18**, 755.
8   E. V. Lenthe, J. G. Snijders and E. J. Baerends, *J. Chem. Phys.*, 1996, **105**, 6505.
9   Z. Y. Liu, T. Lu, Q. X. Chen, *Carbon*, 2020, **165**, 461.
10 J. L. Bre´das, J. P. Calbert, D. A. da Silva Filho and J. Cornil, *Proceedings of the National Academy of Sciences*, 2002, **9**, 5804.
11 C. Lefebvre, G. Rubez, H. Khartabil, J. C. Boisson, J. C. García and E. Hénon, *Phys. Chem. Chem. Phys.*, 2017, **19**, 17928.
12 W. Humphrey, A. Dalke and K. Schulten, *J. Mol. Graph.*, 1996, **14**, 33.